LBL-37323
UC-414

Lawrence Berkeley Laboratory
UNIVERSITY OF CALIFORNIA

Accelerator & Fusion Research Division

Presented at the International Symposium of Heavy Ion Inertial Fusion, Princeton, NJ, September 6–9, 1995, and to be published in the Proceedings

Emittance Growth from Merging Arrays of Round Beamlets

O.A. Anderson

August 1995

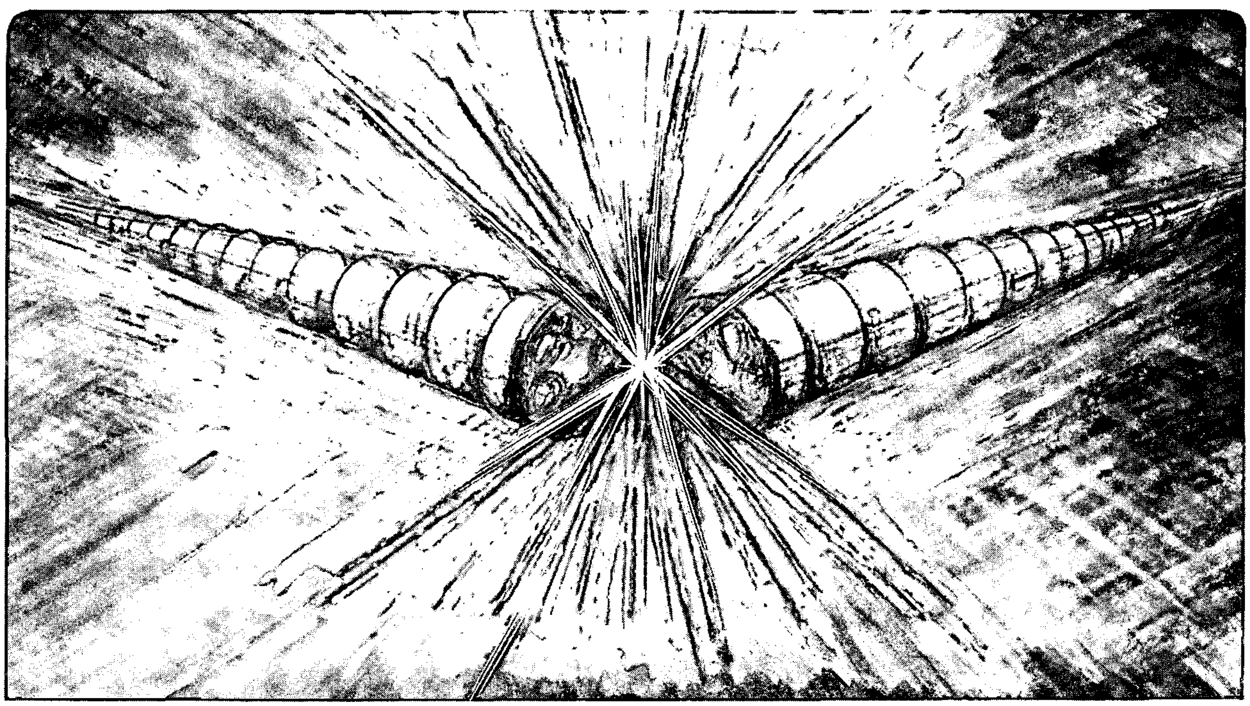

Prepared for the U.S. Department of Energy under Contract Number DE-AC03-76SF00098

LBL-37323
UC-414

Emittance Growth from Merging Arrays of Ground Beamlets

O.A. Anderson

Accelerator and Fusion Research Division
Lawrence Berkeley National Laboratory
University of California
Berkeley, California 94720

August 1995

This work was supported by the Director, Office of Energy Research, High Energy Physics Division, of the U.S. Department of Energy under Contract No. DE-AC03-76SF00098.

EMITTANCE GROWTH FROM MERGING ARRAYS OF ROUND BEAMLETS

O. A. ANDERSON

Lawrence Berkeley National Laboratory

The cost of an induction linac for Heavy Ion Fusion (HIF) may be reduced if the number of channels in the main accelerator is reduced. There have been proposals to do this by merging beamlets (perhaps in groups of four) after a suitable degree of preacceleration. In the process of merging, space charge forces cause transverse acceleration, filling in the gaps and rapidly increasing the emittance. The maximum change in mean-square emittance is proportional to the excess electrostatic energy (free energy) in the array when the merging begins.

In some designs, it may be desirable to reduce the emittance growth below that produced by a basic 2x2 array. For this, a general understanding is helpful. Therefore, we investigate three factors affecting the normalized free energy U_n of an array of charged interacting beamlets: (1) the number of beamlets N in the array; (2) the ratio η of beamlet diameter to beamlet spacing, and (3) the shape of the array. For circular arrays, we obtain an analytic expression showing that $U_n \sim N^{-1}$ in the large-N limit, i.e., the emittance growth can be made arbitrarily small. We show that this is not true for square or rectangular arrays, which have larger free energy with a lower limit determined by the non-circular format. Free energy in square arrays can be reduced by omitting corner beamlets; in the case of a 5x5 array, the reduction factor is as large as 3.3.

I. INTRODUCTION

Free space-charge field energy leads to emittance growth, a fact known since the pioneering analysis by Lapostolle [1] and utilized by Lee, Yu and Barletta [2] in another early contribution. Free energy exists if the initial charge distribution is nonuniform, which is always the case for merging beamlets. Celata et al. [3] analyzed the free energy of a system of four round beamlets located symmetrically within a conducting pipe. More recently, Lee [4] analyzed the general case of N round beamlets having arbitrary currents and positions, with radii also arbitrary except for the restriction that they not overlap. He also obtained an approximation for the case where the conducting pipe is several times larger than the array of N beamlets. With beamlet radii a_i, line charges λ_i, positions δ_i, and array center of mass $\delta \equiv (\sum_i \lambda_i)^{-1} \sum_i \lambda_i \delta_i$, Lee wrote a^2 (twice the mean square radius):

$$a^2 = (\sum_i \lambda_i)^{-1} \sum_i [\lambda_i (a_i^2 + 2\delta_i^2 - 2\delta^2)], \tag{1}$$

and found the free energy

$$U_f = \frac{1}{4\pi\varepsilon_0} \left[\sum_i \lambda_i^2 \ln\frac{a}{a_i} - \sum_j \sum_{i<j} \lambda_i \lambda_j \left(\frac{1}{2} + \ln\frac{|\delta_i - \delta_j|^2}{a^2} \right) \right]. \tag{2}$$

U_f is the difference between the initial field energy and the field energy of a single uniform beam having the same total charge and mean square radius.

We make further analytical progress in Section II by specializing Lee's result to the case of identical beamlets all having the same line charge and radius. This simplification leads to a clear understanding of how the final emittance depends on the initial beam parameters.

Section III analyzes the case of circular arrays, proposed for magnetic fusion injectors [5]. We show that the normalized free energy $U_n \to 4N^{-1}[3/4 - \ln 3\eta + (3/8)\eta^2]$ as N becomes large. This expression is useful even for moderate values of N (e.g., 19). It shows that for any chosen radial occupancy factor η, the free energy can be made arbitrarily low by increasingly fine subdivision. In terms of the number M of rings of beamlets, $U_n \sim M^{-2}$ for large M, the same proportionality as for the case of M sheet beams [6].

Square arrays (§ IV), sometimes proposed for HIF, have configurational free energy which is shown to limit the effect of subdivision and prevent 1/N scaling. In Section V we point out that if a square format is mandated in a large array (e.g. 5x5), then a significant reduction in emittance growth may be obtained by omitting corner beamlets.

II. MERGING IDENTICAL BEAMLETS

In the practical case where all N beamlets have the same line charge λ_0 and radius a_0, Eq. (1) is $a^2 = a_0^2 + 2\langle|\delta_i - \delta|^2\rangle$, the angle brackets indicating an average over all N beamlets. The value of a^2 is independent of the choice of origin and we place the origin at the center of mass:

$$a^2 = a_0^2 + 2\langle\delta_i^2\rangle = a_0^2 + 2\langle x_i^2 + y_i^2\rangle . \tag{3}$$

We write the total line charge as $N\lambda_0 = \Lambda$ and also rearrange terms, so that Eq. (2) becomes

$$U_f = \frac{\Lambda^2}{4\pi\varepsilon_0}\left[-\frac{N-1}{4N} + \frac{1}{2}\ln\frac{a^2}{a_0^2} - \frac{1}{N^2}\sum_j\sum_{i<j}\ln\frac{\delta_{ij}^2}{a_0^2}\right], \tag{4}$$

with notation

$$\delta_{ij}^2 \equiv (x_i - x_j)^2 + (y_i - y_j)^2.$$

Note that both logarithms now have a_0^2 in the denominator, which makes the scaling more obvious. We see from Eqs. (3) and (4) that U_f is invariant to scale, i.e., for a given configuration of beamlets, U_f just depends on the *ratio* of beamlet spacings to beamlet size. Of course, the potential rms emittance growth $\Delta\epsilon$ will depend linearly on the overall scale.

For emittance growth calculations, it is convenient to replace U_f with the normalized free energy U_n, which is obtained by dividing U_f by the self-field energy within a uniform beam having the same rms radius [7]. That is, $U_n = 4U_f(4\pi\varepsilon_0/\Lambda^2)$. Also, the denominators a_0^2 in (4) can be written separately and combined, giving the form used for calculations and for further analysis (App. A):

$$U_n = \frac{4}{N}\left[-\frac{N-1}{4} - \ln a_0 + \frac{N}{2}\ln a^2 - \frac{1}{N}\sum_j\sum_{i<j}\ln\delta_{ij}^2\right]. \tag{5}$$

(Note that U_n, like U_f, is invariant to scale; the units are irrelevant. U_n is also independent of the line charge.) These equations do not require the arrangement of beamlets to possess any symmetry or regularity, as long as the beamlets do not overlap. In practice, a regular arrangement is chosen, as in the following sections.

Emittance growth

We can approximate the emittance growth $\in$ with a result [7] derived for axisymmetric beams. Our arrays lack this symmetry, but we expect the final merged beam to approach such a state, with the released U_n energy equally proportioned: $\in_x = \in_y = \in$. Then [7] $\Delta\in^2 = -KR^2\Delta U_n/16$. K is the normalized perveance, R the rms radius of the system of beamlets, and $\in$ uses Lapostolle's definition [1]. The maximum change in emittance is approximately

$$\Delta(\in^2) = \frac{K}{16}\left(\langle\delta_i^2\rangle + \frac{1}{2}a_0^2\right)U_n, \tag{6}$$

where we note that $R^2 = a^2/2$ and use Eq. (3). We calculate U_n for particular array shapes in the following sections.

III. ANALYTIC AND CALCULATED RESULTS FOR CIRCULAR ARRAY OF BEAMLETS

We use Eq. (5) to investigate the variation of U_n with N for beamlet arrays of various shapes. We start with circular arrays, proposed for large-scale magnetic fusion energy applications [5]. A prototype with 19 beamlets (in a quasi-circular array) was successfully tested at LBNL [5]. Among various shapes, circular arrays have the lowest configurational free energy. In fact, an array of rings in which the number of beamlets per ring is proportional to radius goes over in the large-N limit to a single beam of uniform density, with $U_n = 0$ by definition.

Such an array, with uniform ring spacing Δ_r, is illustrated in Fig. 1.

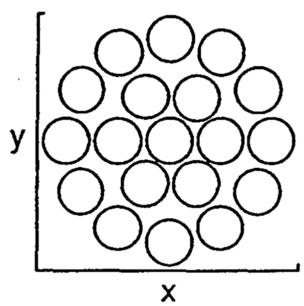

Fig. 1. Array with two rings around a central beamlet; N = 19. At maximum nonoverlapping diameter, most beamlets are in contact with others.

The beamlets will not overlap if $0 < a_0 < \Delta_r/2$. The number of beamlets per ring is proportional to ring radius. For maximum azimuthal density of beamlets, the proportionality factor would be 2π, but for simplicity we use the factor 6. (There is no distinction for $N < 91$.) In the model shown in Fig. 1, the number of beamlets N, including the central beamlet, is related to the number of rings M by

$$N = 1 + 3M(M+1). \tag{7}$$

For convenience, we introduce the filling factor η, defined as the ratio of the actual beam radius to the maximum radius without overlapping:

$$\eta = 2a_0/\Delta_r \quad (0 < \eta < 1). \tag{8}$$

Then, using (7) and (8) we can derive from Eq. (5) our analytic result for large N (Appendix A),

$$U_n \rightarrow \frac{4}{N}\left[\frac{3}{4} - \ln 3 - \ln\eta + \frac{3}{8}\eta^2\right]. \tag{9}$$

Figure 2 plots Eq. (9) as solid lines for the cases $\eta = 0.5$ and $\eta = 1.0$. Also plotted are direct calculations from Eq. (5), listed in Table 1. The total number of beamlets ranges from 7 to 4921, with N extended beyond the range of practical interest to show how the results of (5) approach the asymptotic results of (9). This approach is indicated both in Fig. 2 and in the NU_n columns in Table 1, where the values tend toward the limits 0.1056 and 1.7531 obtained from (9).

Table 1. U_n—from Eq. (5)—and NU_n vs. total number of beamlets for sets of circular arrays.

Rings M	Beamlets N	U_n $\eta = 1.0$	NU_n $\eta = 1.0$	U_n $\eta = 0.5$	NU_n $\eta = 0.5$
1	7	0.011602	0.0812	0.207041	1.4493
2	19	0.006445	0.1224	0.088158	1.6750
3	37	0.003357	0.1242	0.046597	1.7241
4	61	0.001993	0.1216	0.028533	1.7405
5	91	0.001306	0.1189	0.019201	1.7473
6	127	0.000918	0.1166	0.013784	1.7506
7	169	0.000680	0.1149	0.010368	1.7522
8	217	0.000523	0.1135	0.008079	1.7531
10	331	0.000337	0.1115	0.005299	1.7539
12	469	0.000235	0.1102	0.003740	1.7541
15	721	0.000151	0.1089	0.002433	1.7541
20	1261	0.000085	0.1078	0.001391	1.7540
25	1951	0.000055	0.1071	0.000899	1.7538
30	2791	0.000038	0.1067	0.000628	1.7537
35	3781	0.000028	0.1065	0.000464	1.7536
40	4921	0.000022	0.1063	0.000356	1.7535

From (7) and (9), $U_n \sim 1/M^2$ for large M. It is interesting to compare the sheet beam case, where instead of rings of beamlets one has continuous sheets of current. For M current sheets with initial widths equal to the gaps (i.e. $\eta = 0.5$), we found [6]

$$U_n(\text{sheet beams}) = 2 - \frac{2}{M}\,\frac{2M^2 - 1}{(4M^2 - 3)^{1/2}}, \tag{10}$$

and it turns out that for $M > 3$, to good accuracy, $U_n = 1/(4M^2)$. See Table 2.

Table 2. U_n and $M^2 U_n$ vs. number M of rings or sheet beam segments; $\eta = 0.5$.

M	U_n (beamlets)	M^2U_n	U_n(sheets)	M^2U_n
2	0.088158	0.353	0.05855	0.2342
3	0.046597	0.419	0.02712	0.2441
5	0.019201	0.480	0.00992	0.2480
10	0.005299	0.530	0.00250	0.2495
20	0.001391	0.556	0.00062	0.2499
30	0.000628	0.566	0.00028	0.2499
40	0.000356	0.570	0.00016	0.2500

It is not surprising that both cases have the same large-M proportionality. A circular array of round beams can expand radially inward and outward, releasing free electrostatic energy in the

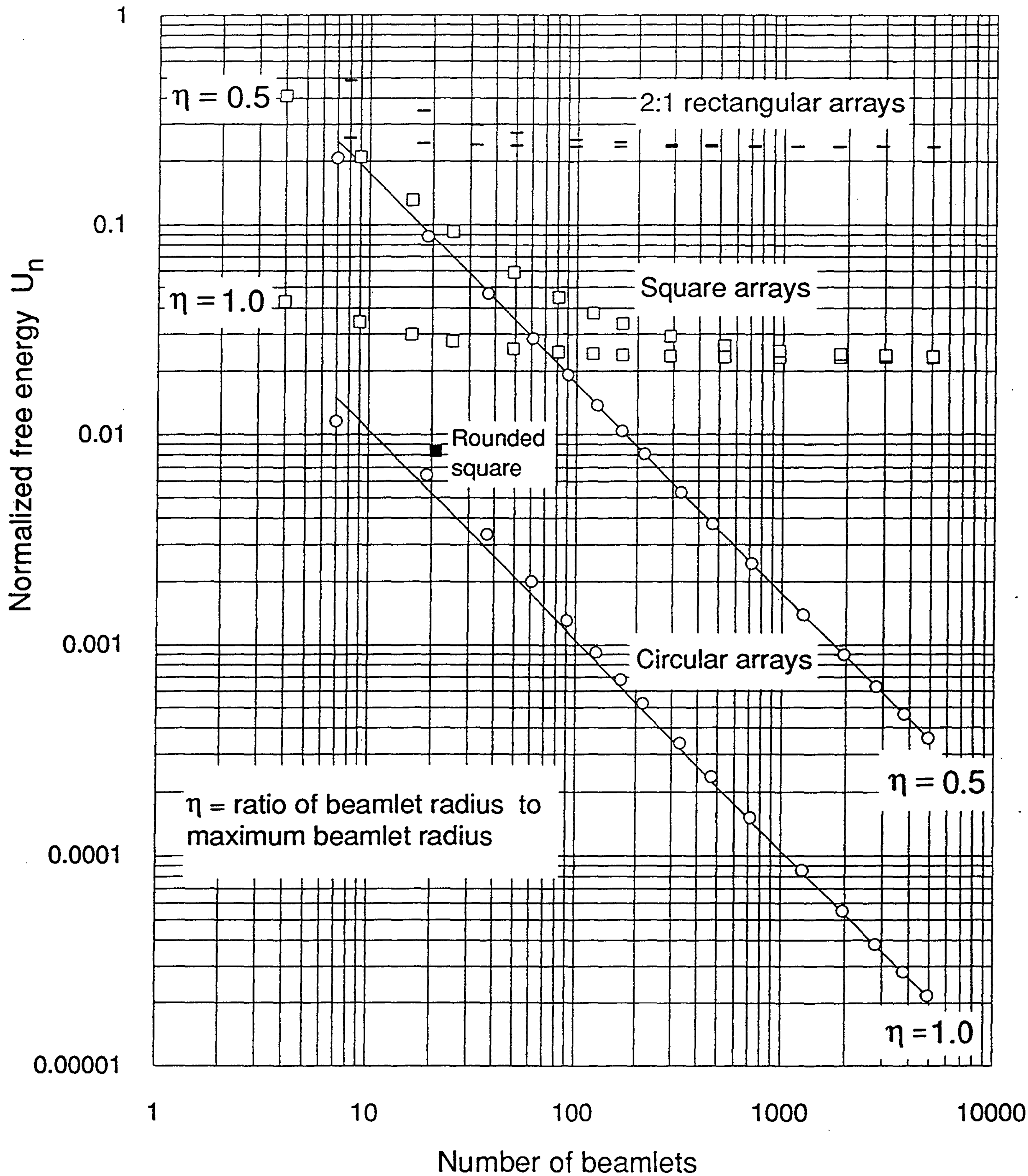

Fig. 2. Normalized free energy vs. N from Eq. (5), showing asymptotic behavior. Solid lines from Eq. (9).

same way as in the sheet beam case. (The individual beamlets also expand azimuthally, which helps to make the emittance growth isotropic.)

IV. SQUARE ARRAYS OF BEAMLETS

Square arrays (4x4) have been proposed for HIF accelerator experiments [8]. However, square arrays produce configurational emittance growth because their shape does not minimize the free energy U_n for a given number of beamlets. Increasing the number of beamlets gives limited improvement in U_n. The free energy asymptotically approaches a value obtained by integration over a uniform square distribution of space charge. This is seen in Table 3 and Fig. 2, where U_n was calculated from Eq. (5). The subdivision has been extended to large numbers to show that U_n is asymptotically independent of N or η, depending only on the overall shape.

Table 3. U_n vs. number of beamlets N in square array, with N extended to show the asymptotic behavior.

Nx	Ny	N	U_n, η=1	U_n, η=0.5
2	2	4	0.04286	0.41097
3	3	9	0.03427	0.20944
4	4	16	0.02992	0.13047
5	5	25	0.02765	0.09257
7	7	49	0.02552	0.05889
9	9	81	0.02460	0.04485
11	11	121	0.02412	0.03770
13	13	169	0.02384	0.03357
17	17	289	0.02355	0.02924
23	23	529	0.02336	0.02647
31	31	961	0.02325	0.02496
43	43	1849	0.02319	0.02408
55	55	3025	0.02316	0.02371
71	71	5041	0.02315	0.02347

Emittance growth

Various scenarios are possible, depending on what is held constant. As one example, let us assume that a given total line charge with a given radius is to be accelerated in one channel of the main accelerator and that this line charge is so large that it is necessary to divide it among at least four pre-accelerator channels—more than four are optional. We also assume that the rms radius R of the pre-merged array is adusted to match the given merged radius so that R in Eq. (6) does not vary. Then various subdivisions affect the emittance growth only through U_n.

It is clear from Fig. 2 that the radial packing fraction η plays an important role. With square arrays, U_n falls off rapidly from the 2x2 value as N increases for the case $\eta = 0.5$ but not for $\eta = 1.0$. With $\eta = 0.5$, a 3x3 array cuts U_n in half according to Table 3; the same result can be obtained with only 7 beamlets in a circular (hexagonal) array—see Table 1. A 4x4 square array has about 1/4 the free energy of the 2x2 array, and the emittance growth is cut in half.

It is more important to achieve large occupancy: if $\eta \rightarrow 1$, the free energy is reduced by a factor of 10 for the 2x2 case. With $\eta = 1.0$, there is little further improvement from subdividing into 3x3 or 4x4 arrays, because the square shape dominates the emittance growth. However, the seven-beamlet hexagonal shape does reduce U_n by an additional factor of four.

Other scenarios exist. For example, one might suppose that the preaccelerated beamlets have predetermined line charges and radii, so that the merged-beam parameters vary with the number of beamlets. Or, one might consider additional mergings after further acceleration. There is not enough space here to discuss all these possibilities.

V. OTHER SHAPES OF ARRAYS

Rectangular Array

Fig. 2 includes the case of rectangular arrays with a 2:1 ratio. This configuration has asymptotic free energy about 10 times larger than for the square configuration, so that there is almost no benefit from subdividing or from increasing η. A wide, thin array could be merged without much emittance growth by using a type of focusing that maintains a ribbon shape, but this would not be feasible for inertial fusion.

Square Array with Rounded Corners

The ideal ring-type configuration of Section III is feasible for MFE sources and pre-accelerators [5], but probably not for HIF where merging is done with septums, tending to produce square arrays. In such cases, omitting corner beamlets can be advantageous. For example, a 5x5 array with ideally thin septums ($\eta \to 1.0$) would decrease its U_n by a factor of 3.3 with the elimination of 4 beamlets. This case is included in Fig. 2, where removing the corners is seen to lower U_n almost to the circular-beam region.

APPENDIX A

Here we derive Eq. (9), which gives the normalized free energy for a round array of beamlets arranged as in Fig. (1). We consider Eq. (5) term by term.

Term 1: Using Eq. (7), we have

$$-\frac{N-1}{4} = -\frac{3}{4}M^2 - \frac{3}{4}M. \tag{A1}$$

Term 2: As noted under Eq. (5), U_n is invariant to change of scale, so that we can choose ring spacing $\Delta_r = 1$. Then (8) becomes

$$\eta = 2a_0 \tag{A2}$$

and

$$-\ln a_0 = -\ln\frac{\eta}{2}. \tag{A3}$$

Term 3: Each ring has radius $\delta_m = m\Delta_r = m$. In our model (Fig. 1), each ring has 6m beamlets, so that in (3)

$$2\langle\delta_i^2\rangle = \frac{2}{N}\sum_{m=1}^{M} 6m\cdot m^2 = \frac{12}{N}\frac{M^2(M+1)^2}{4} = \frac{M^2(1+M^{-1})^2}{1+M^{-1}+3^{-1}M^{-2}},$$

using (7).

$$\ln 2\langle\delta_i^2\rangle = 2\ln M + 2\left(\frac{1}{M} - \frac{1}{2M^2} + \cdots\right) - \left(\frac{1}{M} + \frac{1}{3M^2} - \frac{1}{2M^2} + \cdots\right)$$

$$= 2\ln M + \frac{1}{M} - \frac{5}{6}\frac{1}{M^2} + \cdots .$$

From (3), (A2), and (7)

$$\frac{N}{2}\ln(a^2) = \frac{N}{2}\ln\left(2\langle\delta_i^2\rangle + \frac{\eta^2}{4}\right) = \frac{N}{2}\ln 2\langle\delta_i^2\rangle + \frac{N}{2}\ln\left(1 + \frac{\eta^2}{8\langle\delta_i^2\rangle}\right)$$

$$= N\ln M + \frac{3}{2}M^2\left(1 + \frac{1}{M} + \frac{1}{3M^2}\right)\frac{1}{M}\left(1 - \frac{5}{6}\frac{1}{M}\cdots\right) + \frac{N}{2}\frac{\eta^2}{8\langle\delta_i^2\rangle} + \cdots$$

$$= N\ln M + \frac{3}{2}M + \frac{1}{4} + \cdots + \frac{3}{8}\eta^2 + \cdots. \tag{A4}$$

<u>Term 4</u>: In the double sum, we may specify that the beamlet numbers increase with increasing ring radius. Then beamlet j in ring m interacts with other beamlets $i<j$ of three classes: (a) the central beamlet [Fig. 1]; (b) other beamlets in the same ring m, and (c) beamlets in rings n of smaller radius than m.

$$\sum_j\sum_{i<j}\ln(\delta_{ij}^2) = \sum_{m=1}^{M}[\,\mathrm{sum}_a + \mathrm{sum}_b + \mathrm{sum}_c\,]. \tag{A5}$$

We now evaluate these three sums.

$$\mathrm{sum}_a = 6m\ln m^2 = 12m\ln m. \tag{A6}$$

$$\mathrm{sum}_b = \sum_j\sum_{i<j}\ln\delta_{ij}^2 = 6m\,\frac{1}{2}\sum_{p=1}^{6m-1}\ln m^2\left[\sin^2\frac{p\pi}{3m} + \left(1-\cos\frac{p\pi}{3m}\right)^2\right]$$

$$= 6m\sum_{p=1}^{6m-1}\ln m\,2\sin\frac{p\pi}{6m}$$

$$= 6m\left((6m-1)\ln m + \ln\prod_{p=1}^{6m-1}2\sin\frac{p\pi}{6m}\right);$$

with the identity [9] $\prod_{r=1}^{s-1}2\sin\frac{r\pi}{s} = s$, we have finally

$$\mathrm{sum}_b = 6\,[(6m^2-m)\ln m + m\ln 6m\,]. \tag{A7}$$

Next, using lable k for beamlets in ring n and lable p for beamlets in m,

$$\mathrm{sum}_c = \sum_{n=1}^{m-1}\sum_{p=1}^{6m}\sum_{k=1}^{6n}\ln\delta_{kp}^2. \tag{A8}$$

To evaluate this, we observe that the angle differences between beamlets in rings m and n occur in multiples of $2\pi/6mn$ and then twice use the following identity [9]:

$$\prod_{r=1}^{s}\left[a^2 + b^2 - 2ab\cos\left(\theta + \frac{2r\pi}{s}\right)\right] = a^{2s} + b^{2s} - 2a^sb^s\cos s\theta.$$

We have

$$\sum_{p=1}^{6m}\sum_{k=1}^{6n} \ln \delta_{kp}^{\ 2} = 6\sum_{p=1}^{m} \ln\prod_{k=1}^{6n} \left[m^2 + n^2 - 2mn\cos\left(\frac{k\pi}{3n} - \frac{p\pi}{3mn}\right)\right]$$

$$= 6\sum_{p=1}^{m} \ln \left[m^{12n} + n^{12n} - 2m^{6n}n^{6n}\cos\left(6n\frac{p\pi}{3mn}\right)\right]$$

$$= 6 \ln \left[m^{6mn} - n^{6mn}\right]^2 = 72\, mn \ln m + 12 \ln \left[1 - \left(\frac{n}{m}\right)^{6mn}\right],$$

which is exact so far. The last term is $-12\,(n/m)^{6mn} + \cdots = -12\,[2^{-12} + O(10^{-6})]$ for $m \geq 2$. After doing the sum over n from 1 to m–1 in (A8), we have

$$\text{sum}_c = 6\,[\,6\,m^2(m-1)\ln m - 2^{-11} - O(10^{-6})] \tag{A9}$$

for $m \geq 2$. Inserting (A6), (A7) and (A9) in (A5), we have for Term 4 of Eq. (5)

$$-\frac{1}{N}\sum_j\sum_{i<j} \ln \delta_{ij}^{\ 2} = -\frac{6}{N}\sum_{m=1}^{M} \left[6(m^3 + \frac{m}{3}) \ln m + m \ln 6 - 2^{-11} - \cdots\right]$$

$$= -\left(N - \frac{3}{10N}\right)\ln M + \frac{9}{4}\frac{M^4}{N} - \frac{9}{4}\frac{1}{N} - \frac{N-1}{N}\ln 6 - \frac{6M}{N}2^{-11} + \cdots, \tag{A10}$$

where we used Eq. (7) for the ln 6 term and summed $(m^3 + m/3)\ln m$ with the formula [10]

$$\sum_{x=1}^{M} f(x) = \int_1^M f(x)dx + \frac{1}{2}\left[f(M) + f(1)\right] + \frac{1}{12}\left[f'(M) - f'(1)\right] - \frac{1}{720}\left[f'''(M) - f'''(1)\right] + \cdots.$$

In the second term of (A10) we find $M^4/N = (M^2/3)(1 - M^{-1} + (2/3)M^{-2} + \cdots)$, using Eq. (7) again. Then (A10) becomes, in the limit of large M and N,

$$-\frac{1}{N}\sum_j\sum_{i<j} \ln \delta_{ij}^{\ 2} \longrightarrow -N \ln M + \frac{3}{4}M^2 - \frac{3}{4}M + \frac{1}{2} - \ln 6. \tag{A11}$$

Adding (A1), (A3), (A4) and (A11) then gives Eq. (9).

ACKNOWLEDGMENTS

I thank Edward Lee for discussions that led to this paper and for additional comments. This work was supported in part by U.S. DOE Contract DE-AC03-76SF00098.

REFERENCES

[1] P.M. Lapostolle, Energy Relationships in Continuous Beams, CERN report CERN-ISR-DI/71-6 (1971).

P.M. Lapostolle, Possible Emittance Increase Through Filamentation Due to Space Charge in Continuous Beams, *IEEE Trans. Nucl. Sci.* 18 (1971) 1101.

[2] E.P. Lee, S.S. Yu, and W.A. Barletta, Phase Space Distortion of a Heavy-Ion Beam Propagating Through a Vacuum Reactor Vessel, *Nucl. Fusion* 21 (1981) 961.

[3] C.M. Celata, A. Faltens, David L. Judd, L. Smith, and M.G. Tiefenback, Transverse Combining of Nonrelativistic Beams in a Multiple Beam Induction Linac, *Proc. 1987 Particle Accelerator Conference*, p. 1167; also, personal communication, 1993.

[4] E.P. Lee, personal communication (1993).

[5] O.A. Anderson, W.S. Cooper, W.B. Kunkel, K.N. Leung, A.F. Lietzke, C.F.A. van Os, L. Soroka, J.W. Stearns, and R.P. Wells, Negative Ion Source and Accelerator Systems for Neutral Beam Injection in Large Tokamaks–Part A, Plasma Physics and Controlled Nuclear Fusion Research 1990 (International Atomic Energy Agency, Vienna, 1991) Vol. 3, p. 503.

J.W. Kwan, et al., *Rev. Sci. Intrum.* 66 (1985) 3864.

[6] O.A. Anderson, Internal Dynamics and Emittance Growth in Space-Charge-Dominated Beams, *Particle Accelerators* 21 (1987) 197.

[7] T.P. Wangler, K.R. Crandall, R.S. Mills, and M. Reiser, Relation between Field Energy and RMS Emittance in Intense Particle Beams, *IEEE Trans. Nucl. Sci.* 32 (1985) 2196.

[8] ILSE Conceptual Engineering Design Study, Lawrence Berkeley Laboratory PUB-5219 (1989) p. 35.

[9] Z.A. Melzak, Companion to Concrete Mathematics (Wiley, New York, 1973) p. 99.

[10] H.T. Davis, The Summation of Series (Principia Press, San Antonio, 1962) p. 49.

LAWRENCE BERKELEY NATIONAL LABORATORY
UNIVERSITY OF CALIFORNIA
TECHNICAL & ELECTRONIC INFORMATION DEPARTMENT
BERKELEY, CALIFORNIA 94720